Pergamon

Atmospheric Environment Vol. 30, No. 7, pp. 1167–1176, 1996

1352-2310/96 $15.00 + 0.00

1352-2310(95)00248-O

THE EFFECT OF STEADY WINDS ON RADON-222 ENTRY FROM SOIL INTO HOUSES

W. J. RILEY,*,† A. J. GADGIL,†,‡ Y. C. BONNEFOUS§ and W. W. NAZAROFF*

*Civil Engineering Department, University of California, Berkeley, CA 94720, U.S.A.; †Indoor Environment Program, Lawrence Berkeley National Laboratory, Berkeley, CA 94720, U.S.A.; and §Groupe Informatique et Systemes Energetiques, Ecole Nationale des Ponts et Chaussees, Central 2, La Courtine, 93167 Noisy-Le-Grand Cedex, France

(*First received* 4 *November* 1994 *and in final form* 3 *June* 1995)

Abstract—Wind affects the radon-222 entry rate from soil into buildings and the resulting indoor concentrations. To investigate this phenomenon, we employ a previously tested three-dimensional numerical model of soil-gas flow around houses, a commercial computational fluid dynamics code, an established model for determining ventilation rates in the presence of wind, and new wind tunnel results for the ground-surface pressure field caused by wind. These tools and data, applied under steady-state conditions to a prototypical residential building, allow us (1) to determine the complex soil-gas flow patterns that result from the presence of wind-generated ground-surface pressures, (2) to evaluate the effect of these flows on the radon concentration in the soil, and (3) to calculate the effect of wind on the radon entry rate and indoor concentration. For a broad range of soil permeabilities, two wind speeds, and two wind directions, we quantify the "flushing" effect of wind on the radon in the soil surrounding a house, and the consequent sharp decrease in radon entry rates. Experimental measurements of the time-dependent radon concentration in soil gas beneath houses confirm the existence of wind-induced flushing. Comparisons are made to modeling predictions obtained while ignoring the effect of the wind-generated ground-surface pressures. These investigations lead to the conclusion that wind-generated ground-surface pressures play a significant role in determining radon entry rates into residential buildings.

Key word index: Radon, wind, indoor air quality, contaminant transport, soil-gas transport.

NOMENCLATURE

A_i	cross-sectional area of a portion of the footer-slab crack, m^2
A_l	effective leakage area, m^2
A_w	surface-area element of the house's exterior wall, m^2
$c_p(x, y)$	ground-surface pressure coefficient at location (x, y), dimensionless
c	Forchheimer term, $s\,m^{-1}$
C	radon soil-gas concentration, $Bq\,m^{-3}$
C_{in}	indoor radon concentration normalized with respect to C_∞, dimensionless
C_{char}	spatial average of the radon soil-gas concentration normalized with respect to C_∞, dimensionless
C_∞	deep-soil radon concentration in soil gas, $Bq\,m^{-3}$
D	diffusivity of radon through bulk soil, $m^2\,s^{-1}$
D_w	product of the average wall permeability times the area of the wall, $m^3\,s^{-1}\,Pa^{-n}$
E	normalized radon entry rate into the basement, $m^3\,s^{-1}$
f_w	local terrain constant, dimensionless
k	soil permeability, m^2
n	flow exponent, dimensionless
p	disturbance pressure, Pa
$p_{gs}(x, y)$	ground-surface pressure at location (x, y), Pa
p_∞	free-stream air pressure, Pa
p_i	pressure inside the building, Pa
p_w	exterior pressure on an element of the house wall, Pa
ΔP	pressure difference across a section of the house wall, Pa
Q	ventilation flow rate, $m^3\,s^{-1}$
Q_i	air flow rate into or out of the building through a section of the exterior wall, $m^3\,s^{-1}$
Q_{sg}	soil-gas flow rate into the house, $m^3\,s^{-1}$
$Q_{s,uv}$	ventilation flow from the stack effect and unbalanced ventilation, $m^3\,s^{-1}$
S	production rate of radon in the soil gas, $Bq\,m^{-3}\,s^{-1}$
V_{eh}	wind speed at eave height, $m\,s^{-1}$
$\mathbf{v}$	soil-gas velocity vector, $m\,s^{-1}$

Greek letters

α	empirically determined constant used in the footer-slab crack model, $m^3\,s\,kg^{-1}$
β	empirically determined constant used in the footer-slab crack model, $s\,m^{-1}$
ε	porosity of the soil, dimensionless
λ	radon-222 decay constant, $2.1 \times 10^{-6}\,s^{-1}$
μ	dynamic viscosity of air, $kg\,m^{-1}\,s^{-1}$
ρ	air density, $kg\,m^{-3}$

‡Author to whom correspondence should be addressed.

INTRODUCTION

The recognition that indoor radon is a serious health concern has resulted in a substantial effort to elucidate the factors that determine both its entry rate into buildings and its indoor concentrations. Detailed studies, both experimental and numerical, have investigated the effects of environmental conditions, building characteristics (such as the presence of a basement or crawlspace), and the operation of mechanical ventilation systems and furnaces on radon entry into buildings. Insights from this research have led to numerical models designed to predict radon entry rates into buildings for simple, well characterized soils, and under relatively stable meteorological conditions.

Advective entry of radon-bearing soil gas is the dominant source of indoor radon in most homes with elevated concentrations (Nazaroff, 1992). In buildings with basements, a small depressurization is sufficient to drive soil gas through cracks in the substructure (such as the joints between the footer and basement slab running along the periphery of the basement). The driving force for this entry is the small indoor–outdoor pressure difference (on the order of 1–10 Pa) which can be generated by indoor–outdoor temperature differences, space conditioning equipment, mechanical exhaust, transient changes in barometric pressure, and the interaction of wind with the building structure. Among these, wind is unique since, in addition to depressurizing the building, it alters the pressure profile on the ground-surface adjacent to the building. This wind-induced ground-surface pressure field influences soil-gas flow, thereby altering the radon concentration in the soil gas surrounding the building. As summarized below, evidence suggesting that wind can play a role in determining the amount of radon that enters a house has been presented elsewhere. Little has been published, however, with the intent of quantifying this role and understanding the mechanisms involved.

Passive or low-energy radon mitigation systems can also be influenced by wind (Fisk *et al.*, 1995). The effects are especially pronounced when a direct connection between the atmosphere and sub-slab gravel layer is present. Design of these systems will need to account for both the effect of wind on soil-gas concentrations and on the method of coupling the gravel layer to the outdoors.

A striking example of the effects of wind on radon entry rates and indoor concentrations was presented by Turk *et al.* (1990). Figure 1 reproduces their data for a house in the Pacific Northwest showing a strong inverse correlation between wind speed and indoor radon concentration. Although some of the decrease in the indoor radon concentration with increasing wind speed is due to increased ventilation, this factor is not large enough to account for the full reduction shown. A concurrent reduction in the radon entry rate must also have occurred. The authors hypothesized

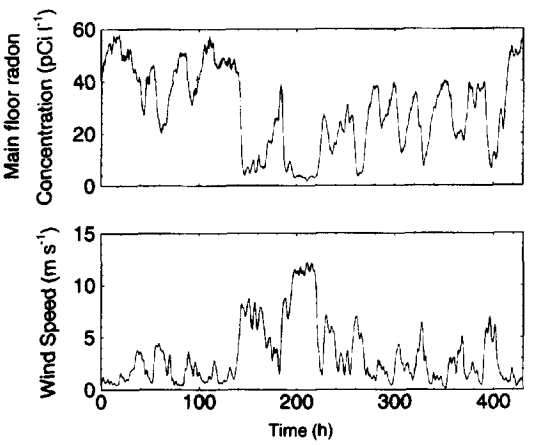

Fig. 1. Indoor radon concentration and wind speed measured over a three-week period at ESP111 (Spokane, WA) from the study by Turk *et al.* (1990). Note the inverse correlation between wind speed and indoor concentration, and the magnitude of the reduction in indoor concentration during the periods of high wind speeds. The data were collected between 23 November and 11 December 1985.

that the wind ventilated the soil surrounding the house, thus reducing the soil-gas radon available for entry into the building. In the *Results* section of this paper we present direct experimental evidence of soil-gas flushing at several test houses in New Jersey, and indicate that this depletion follows the trends predicted in our numerical simulations.

Nazaroff *et al.* (1985) instrumented a house in Illinois to monitor the effects of various environmental factors on radon entry rates. They concluded that when the indoor–outdoor temperature difference was small, high wind speeds were associated with higher radon entry rates, and conversely, when this temperature difference was large, low wind speeds produced higher radon entry rates. They also noticed a correlation between high wind speeds and decreased radon concentrations in the soil gas, possibly as a result of the flushing of radon from the soil gas. Their observations did not lead to conclusive elucidation of the mechanisms responsible for these relationships.

Arnold (1990) conducted an experiment with a three-dimensional scale model of a house, and imposed on the ground surface a simplified version of the wind-induced ground-surface pressure distribution reported by Scott (1985). Resulting perturbations of the pressure field in the porous medium used to represent the soil were then measured. However, radon concentrations in the ersatz soil were not measured, and therefore the effect of wind on radon entry rates into the basement was not determined. Ward *et al.* (1993), in their experimental study of a small building structure, observed a correlation between wind speed and the pressure difference between indoor air and the soil gas. However, the above-ground structure in these experiments is not geometrically similar to a real house. It is therefore difficult to

extend these correlations to full-scale houses, which are affected by both wind-induced depressurization and the ground-surface pressure field.

Scott (1985) reported a numerical investigation of the effects of wind speed and direction on radon entry rates using a finite-element model of a simple building. Ground pressure data generated in a small wind tunnel and meteorological data from a summer and winter period in Toronto were used as input to the simulations. Their simulations predicted that both wind speed and wind direction affect the radon entry rate into a building, but they found no simple correlation among these factors. Sherman (1992) developed a simplified model of a house to quantify the effects of several factors, including wind, on radon entry. Sherman assumed that the wind did not deplete the soil gas of radon, but did increase the ventilation rate and basement depressurization. He concluded that the stack effect is much more effective at inducing radon entry than is the wind effect. Owczarski *et al.* (1991) performed a numerical study of the effects of wind and reported expected reductions in the soil-gas radon concentration below a slab-on-grade house. However, that study ignored crucial details of building structure (e.g. existence of footers), did not consider the full two-dimensional nature of the wind-generated ground-surface pressure field, used arbitrary values for wind-generated ground-surface pressures, and considered only Darcy flow through the soil and gravel layer.

Taken in combination, these efforts do not yield a comprehensive picture of how wind affects radon entry rates and indoor concentrations. We aim to improve our understanding by reporting on a detailed investigation of wind-induced radon entry into a prototypical residential building under steady-state conditions. This study particularly emphasizes two issues: the effect of wind-induced ground-surface pressures on the soil-gas radon concentration near a house, and the interplay between ventilation and radon entry in affecting indoor concentrations when both are driven by wind. To pursue these objectives, we employ a largely numerical approach, combining three modeling tools with new wind tunnel data of the ground-surface pressure field induced by wind blowing on a building. The modeling tools comprise (1) a previously tested, three-dimensional finite-difference model, known as non-Darcy STAR (NDSTAR), of soil-gas flow and radon concentrations around buildings (Gadgil *et al.*, 1991; Bonnefous *et al.*, 1992); (2) a commercial computational fluid dynamics code, FLUENT (FLUENT, 1993); and (3) a model for determining the house ventilation rate in the presence of wind (Sherman, 1992). We also present previously acquired but unpublished experimental data that qualitatively substantiates key model predictions. Although the methods employed are general, the modeling results reported in this paper apply specifically to radon-222, the isotope responsible for the dominant portion of human exposure.

METHODS

Overview

The simulation of the wind's interaction with the building and surrounding soil was carried out in a five-step process. First, results from recent wind tunnel experiments were used to compute the wind-generated ground-surface pressure field around the house. Second, the wind-induced depressurization in the house was calculated from FLUENT's predictions of the distribution of pressures on the exposed walls. Third, the pressure and velocity fields in the soil gas surrounding the house and in the subslab gravel layer were computed using NDSTAR. Fourth, the soil-gas radon concentration field was determined and a radon entry rate into the house was calculated. Finally, the indoor radon concentration was computed using a predicted wind-induced enhancement of the building's ventilation rate. This five-step exercise, which is described in more detail below, was carried out for a range of soil permeabilities, two wind speeds, and two wind directions.

A central approximation in this study is that wind establishes a steady-state ground-surface pressure field, depressurization of the house, and flow of soil gas and radon. In reality, both wind speed and direction vary with time. Over the range of soil permeabilities we will consider, the soil-gas pressure field will reach a steady state after a perturbation with a characteristic time of seconds to minutes (Nazaroff *et al.*, 1988). The soil-gas concentration field will reach a steady state with a characteristic time that is the smaller of (1) the time soil gas takes to travel from the soil surface to the basement (on the order of hours to months, depending on the soil permeability), and (2) the time required for the radon concentration to reach a steady value as a result of its radioactive generation and decay (several days).

Macrometeorological wind fluctuations typically have peaks in the wind energy distribution at periods on the order of days. In contrast, small-scale wind fluctuations have significant energy at periods on the order of a minute (Van der Hoven, 1957). For the macrometeorological region of the wind spectrum, the soil-gas pressure field is likely to reach steady state. However, because the time required for the radon concentration field to equilibrate can be large, the assumption of a steady soil-gas concentration field is not strictly appropriate, even for large-scale wind fluctuations. Still, the assumption of steady state captures some of the key features of the problem, and is therefore useful as an important step towards full understanding of the effects of wind on radon entry into homes.

House substructure and soil characteristics

The house geometry was chosen to represent a typical single-family structure in size and aspect ratio, but not intended to characterize a statistically "normal" home. The building has a plan area of 8.7 m × 10.4 m; the basement and footers represent standard construction practice and are depicted in Fig. 2a. A 1 mm L-shaped crack provides the route for advective entry of radon into the basement. Advective flow through this channel is modeled with the equation (Baker *et al.*, 1987)

$$\nabla p = \alpha(1 + \beta|\mathbf{v}|)\mathbf{v} \qquad (1)$$

where p is the disturbance pressure (Pa), α and β are empirically determined constants that are functions of the crack geometry, and $\mathbf{v}$ is the soil-gas velocity vector ($\mathrm{m\,s^{-1}}$). For this study α is $860\ \mathrm{kg\,m^{-3}\,s^{-1}}$ and β is $0.035\ \mathrm{s\,m^{-1}}$ (Gadgil *et al.*, 1991).

We varied the permeability of the soil surrounding the house from $1 \times 10^{-11}\ \mathrm{m^2}$ to $1 \times 10^{-8}\ \mathrm{m^2}$. The lower bound was chosen because wind does not significantly affect soil-gas radon concentrations below this value. The upper bound is a permeability above which no houses are expected to be found (Nazaroff, 1992). The permeability of the gravel placed

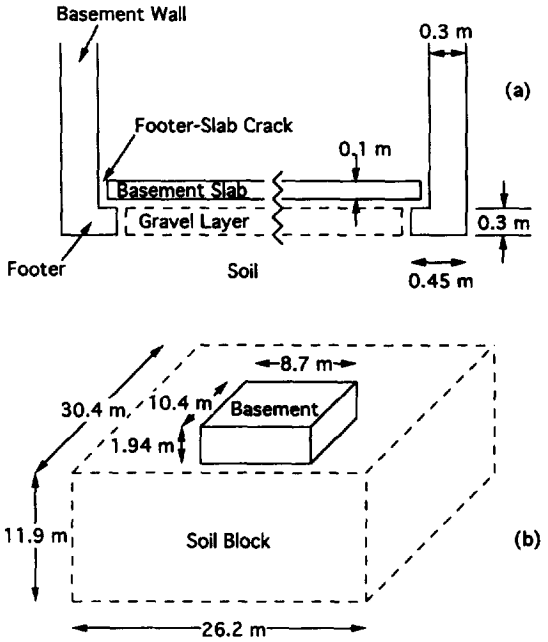

Fig. 2. Geometry of the substructure of the house (a) and the computational space (b). The diagrams are not drawn to scale.

under the basement slab is taken as 3×10^{-7} m^2, corresponding approximately to a 4.5 cm round gravel (Gadgil *et al.*, 1991).

Wind-induced ground-surface pressure field

The pressure field established around a house in the presence of wind was determined by conducting scale experiments in the U.C. Berkeley Architecture Department's wind tunnel facility (see Bauman *et al.*, 1988, for a description of the wind tunnel, and Riley *et al.*, 1995a, for details regarding these experiments). For the results presented here, the house is a box of dimension 8.7 m × 10.4 m × 3 m. The ground-surface pressure coefficient, $c_p(x, y)$, is defined as

$$c_p(x, y) = \frac{p_{gs}(x, y) - p_\infty}{\frac{1}{2}\rho V_{eh}^2} \quad (2)$$

where $p_{gs}(x, y)$ is the ground-surface pressure (Pa) at location (x, y), p_∞ is the free-stream pressure (Pa), ρ is the air density (kg m^{-3}), and V_{eh} is the free-stream wind speed at an eave height of 3 m (m s^{-1}). Figures 3a and b present the ground-surface pressure coefficient field for the case of wind incident perpendicular to the short side of the house and incident at 45° to the side of the house, respectively.

Eave-height wind speeds of 0, 3.6, and 8.3 m s^{-1} are used in combination with equation (2) and the results presented in Fig. 3 to define the ground-surface pressure field for the simulations. The non-zero wind speeds correspond to the 5th and 95th percentile wind speeds, respectively, over a period of approximately 25 years in Spokane, Washington (NOAA, 1980). This location was chosen because radon entry and mitigation has been investigated in several houses in the area (Turk *et al.*, 1990). For comparison, the average wind speed in the U.S. is 4.1 m s^{-1}.

Wind-induced indoor depressurization

The depressurization of the house air can be caused by several factors. We consider only wind-induced depressurization in order to focus attention on the effects of wind on

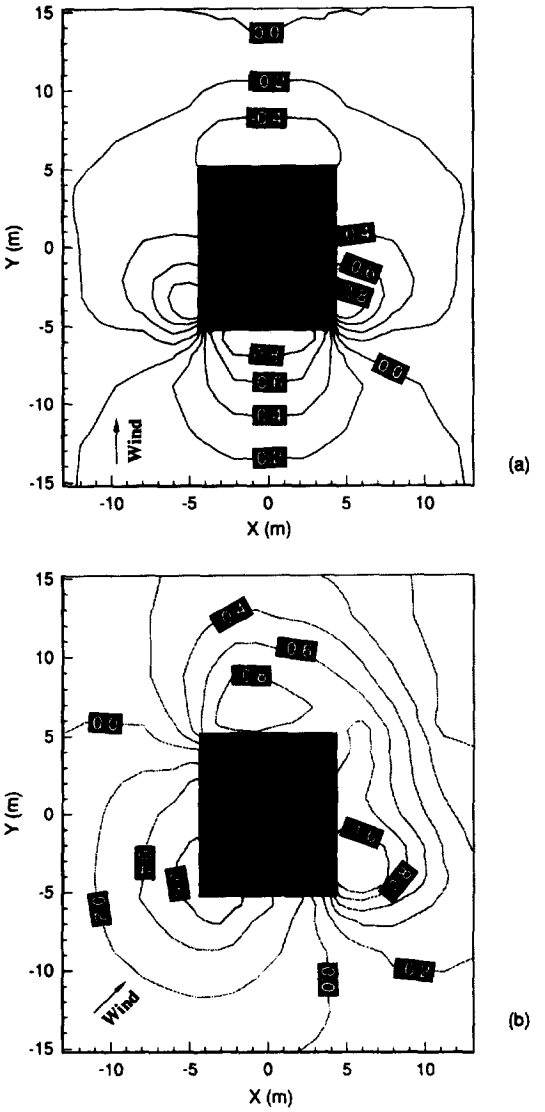

Fig. 3. Contour plot of the ground-surface pressure coefficient (plan view) for wind incident at an angle of 0° (a) and 45° (b) to the house. The pressure coefficient is the fraction of the eave-height (3 m) dynamic pressure of the wind that is felt on the ground surface.

the radon entry rate. Physically, this situation would occur under steady wind conditions when the indoor–outdoor temperature difference is small and no mechanical ventilation or heating equipment is operating. To highlight the importance of including the wind-induced ground-surface pressures, we have performed analogous simulations (same house geometry and range of soil permeabilities) with the ground surface at atmospheric pressure and a basement depressurization of −11 Pa. This is the basement depressurization that we estimate is caused by an 8.3 m s^{-1} wind, as described below.

The indoor depressurization is computed by balancing the total flow into and out of the building (Mowris and Fisk, 1988)

$$Q_i = D_w(\Delta P)^n \quad (3)$$

where Q_i is the air flow rate into or out of the building through the section of the exterior wall being considered (m^3 s^{-1}), D_w is the product of the average wall permeability

times the area of that section of the wall ($m^3 s^{-1}$ Pa), ΔP is the pressure difference across that section of the wall (Pa), and n is a flow exponent. The flow exponent depends on the character of the flow through the cracks: it is 1.0 for flow dominated by viscous forces, and 0.5 for flow dominated by inertial forces. A typical value, integrated over all the cracks in a house, is 0.66 (Sherman *et al.*, 1984). Equation (3) and the requirement that the air mass in the building remain constant gives

$$\sum_{\text{surfaces}} (A_w) * \text{sign}(p_w - p_i) * (p_w - p_i)^n = 0 \qquad (4)$$

where A_w is a surface-area element of the exterior wall (m^2), p_w is the exterior pressure on an element of the house wall (Pa), and p_i is the pressure inside the building (Pa). In deriving equation (4) we have assumed an equal distribution of leakage area around the house and that the building has no mechanical supply or exhaust.

We used FLUENT to determine p_w by solving the conservation equations for mass and momentum in the air flow around the house. FLUENT discretizes the space with a control-volume-based, finite-difference technique, and we used the k–ε model to simulate turbulence. The computational grid included open space a distance of six house dimensions from the building in both horizontal directions, a vertical dimension of 61 m, and was divided into 100,000 control volumes. The building's walls were modeled as smooth surfaces. We have assumed that the house is isolated from other buildings, and that the atmospheric boundary layer corresponds to what might be expected on the outskirts of a small town (see Riley *et al.*, 1995a, for details of this simulation).

Equation (4) is solved iteratively once the values for p_w are determined. With the wind perpendicular to the short side of the house, the interior depressurization is predicted to be -11 Pa for a wind speed of 8.3 m s^{-1}, and -2.0 Pa for a wind speed of 3.6 m s^{-1}.

Because the predicted values of p_i are subject to inaccuracies inherent in the FLUENT simulation, we also computed the building depressurization by the method of Feustel (1985). For the wind speeds given above, we calculate building depressurizations of -13 and -2.4 Pa, respectively. These values are both within 20% of the values computed using FLUENT.

Soil-gas pressure and velocity fields

The soil-gas pressure, velocity, and concentration fields were computed in a soil block that measures 30.4 m × 26.2 m horizontally, and extends 11.9 m below the soil surface (Fig. 2b). There are 40,716 node points in this volume. The exterior surfaces of the soil block are taken to be Neumann boundaries (no flow), as are all interfaces where the soil meets the basement. The Neumann boundary at the bottom of the computational space is equivalent to assuming that an impermeable layer exists at this depth (e.g. water table). Dirichlet boundaries (fixed pressure) are imposed on the ground surface and along the crack that connects the subslab gravel layer with the basement.

The pressure and velocity fields in the soil gas are solved simultaneously using the three-dimensional finite-difference software package NDSTAR (Gadgil *et al.*, 1991; Bonnefous *et al.*, 1992). This package can model both Darcy and non-Darcy flow of soil gas, as appropriate, in regions of gravel and soil. The non-Darcy flow is modeled with the Darcy–Forchheimer equation:

$$\nabla p = -\frac{\mu}{k}(1 + c|\mathbf{v}|)\mathbf{v} \qquad (6)$$

where p is the soil-gas disturbance pressure (Pa), k is the soil permeability (m^2), μ is the dynamic viscosity (kg $m^{-1} s^{-1}$), and c is the Forchheimer term (s m^{-1}). Gadgil *et al.* (1991) describe the experimental procedure used to determine the Forchheimer term.

Since the disturbance pressure is always small relative to atmospheric pressure, the soil gas is treated as incompressible. Therefore, the continuity equation becomes

$$\nabla \cdot \mathbf{v} = 0. \qquad (7)$$

The model assumes that each zone of soil is homogeneous and isotropic, the concrete basement walls and floor are impermeable to soil-gas flow (except through the cracks), and the effect of buoyancy on soil-gas flow is negligible. A modified SIMPLE algorithm (Patankar, 1980) is used to discretize equations (6) and (7), and the pressure and velocity fields are calculated on staggered grids using an alternate direction implicit method. The solution procedure is terminated when the computed pressure at each point changes fractionally by less than 1×10^{-6} over successive iterations.

Soil-gas concentration field

Given the soil-gas velocity field, the radon concentration field is calculated from the steady-state radon mass balance equation

$$\nabla \cdot (D \nabla C) - \nabla \cdot (\mathbf{v}C) + \varepsilon(S - \lambda C) = 0 \qquad (8)$$

where C is the radon concentration in the soil gas (Bq m^{-3}), D is the diffusivity of radon through bulk soil ($m^2 s^{-1}$), S is the emanation rate of radon from soil grains into the soil gas (Bq $m^{-3} s^{-1}$), λ is the radon decay constant (s^{-1}), and ε is the porosity of the soil. In contrast to the pressure and velocity field computations, the ground surface here is represented by a mixed boundary condition because there may be areas (i.e. on the leeward side of the house) where the magnitudes of the advective and diffusive radon flux out of the ground are comparable.

The normalized radon entry rate into the basement is then calculated by summing the flux into the crack over the cross-sectional area of the crack

$$E = \frac{\sum_i C \cdot \mathbf{v} \cdot A_i}{C_\infty} \qquad (9)$$

where E is the normalized radon entry rate into the basement ($m^3 s^{-1}$), A_i is the cross-sectional area (m^2) of the portion of the crack under consideration, C and $\mathbf{v}$ are evaluated at the opening of the crack in the gravel layer, and C_∞ is the radon concentration in the soil gas far below the surface (Bq m^{-3}).

Indoor radon concentration

The normalized, steady-state indoor radon concentration is calculated from the normalized radon entry rate and an estimate of the house's ventilation rate. We use the LBL infiltration model (Sherman, 1992) to estimate the ventilation flow rate, Q ($m^3 s^{-1}$), in the presence of wind:

$$Q = [A_l^2 f_w^2 V_{eh}^2 + Q_{sg}^2 + Q_{s,uv}^2]^{0.5} \qquad (10)$$

where A_l is an effective leakage area (m^2), f_w is a wind parameter equal to 0.23, corresponding to a lightly shielded building (Mowris and Fisk, 1988), Q_{sg} is the soil-gas flow rate into the house ($m^3 s^{-1}$), and $Q_{s,uv}$ is the ventilation flow ($m^3 s^{-1}$) from the stack effect and unbalanced ventilation. Note that for cases with wind, $Q_{s,uv}$ is set to zero, and for cases without wind, V_{eh} is set to zero. We use an effective leakage area of 6.1×10^{-2} m^2. This number was reported by Palmiter and Brown (1989) in their study of Northwest houses as an average value for homes without ducted heating systems.

Table 1 lists the four simulation cases we examined and indicates for each the basement depressurization, house air exchange rate, and whether wind-induced ground-surface pressures are included.

Table 1. Wind conditions, basement depressurization, and air-exchange rate for the four simulation cases

Case	Wind conditions	Basement depressurization (Pa)	Air-exchange rate (h^{-1})	Wind-induced ground-surface pressures
1	None	−11	1.5	No
2	8.3 m s^{-1} at 0°	−11	1.5	Yes
3	8.3 m s^{-1} at 45°	−11	1.5	Yes
4	3.6 m s^{-1} at 0°	−2.0	0.65	Yes

The normalized indoor radon concentration, C_{in}, is calculated as

$$C_{in} = \frac{E}{Q}. \quad (11)$$

The dimensional indoor radon concentration equals the product of C_{in} and C_∞. A typical value for C_∞ is 30 kBq m^{-3} (Nazaroff, 1992).

RESULTS AND DISCUSSION

Radon and soil-gas entry rates

Figure 4b shows predicted normalized radon entry rates as a function of soil permeability for wind speeds of 3.6 and 8.3 m s^{-1} at a wind incidence angle of 0°, and for a wind speed of 8.3 m s^{-1} at a wind incidence angle of 45°. We plot the results for case 1 on a separate graph (Figure 4a) to emphasize that here the ground surface is at atmospheric pressure, although the basement depressurization remains −11 Pa.

The simulation predictions with a uniform ground-surface pressure (case 1) follow a commonly observed pattern over a wide range of house geometries (e.g. Revzan and Fisk, 1992). For soil permeabilities less than about 1×10^{-10} m^2 the radon entry rate increases linearly as soil permeability increases. However, as the soil permeability increases above this value, the radon entry rate begins to level off. The lower resistance to soil-gas flow accompanying the increase in soil permeability causes more of the pressure drop between the basement and the soil surface to occur across the footer-slab crack. The result is a lower driving force for soil-gas movement and hence radon entry. For larger crack sizes, the flow of soil gas into the basement can continue to increase with increasing soil permeability (Mowris and Fisk, 1988). In this case, the radon depletion in the soil gas adjacent to the crack can also be a factor in limiting the radon entry rate at high soil permeabilities.

The predictions that include wind-induced ground-surface pressures (cases 2–4) show a remarkably different dependence on soil permeability. For these cases the radon entry rate peaks at a soil permeability in the range $(1–3 \times 10^{-10}$ m^2; further increases in soil permeability lead to substantially lower radon entry rates. Even at a permeability of 10^{-11} m^2, the radon entry rate is significantly affected when the ground-surface pressure field is included.

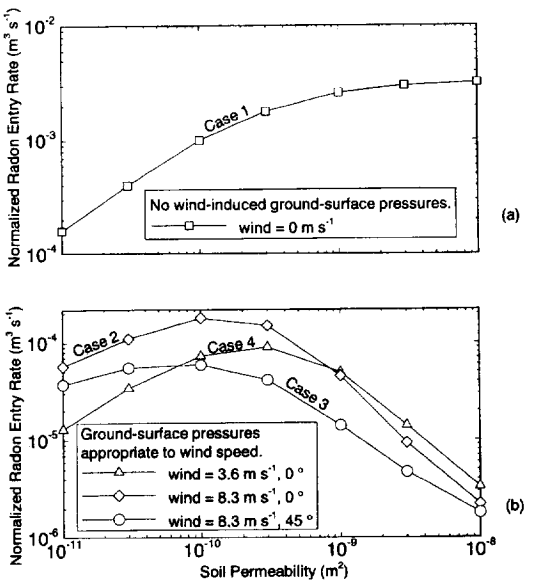

Fig. 4. Normalized radon entry rate from soil gas into the basement as a function of soil permeability. The radon entry rate is normalized with respect to the deep-soil gas-phase radon concentration. The gravel permeability is 3×10^{-7} m^2. The basement depressurization for no wind (i.e. no wind-induced ground-surface pressures) is set at −11 Pa, for the 3.6 m s^{-1} wind it is −2.0 Pa, and for the 8.3 m s^{-1} wind it is −11 Pa. Note the different y-axis scales for Figs 4a and b.

Simulations were also performed with the higher basement depressurizations obtained using the technique of Feustel (1985): −13 Pa for a wind speed of 8.3 m s^{-1} and −2.4 Pa for a wind speed of 3.6 m s^{-1}. The shape of the curves were similar to those shown in Fig. 4, demonstrating that the qualitative effect of wind on the radon entry rate is not a sensitive function of basement depressurization.

Wind-induced flushing of soil-gas radon

A detailed examination of the simulation results reveals the underlying reason for the sharp drop in radon entry rate with increasing soil permeability when the house is exposed to wind. The bulk soil-gas flow under the house that is driven by wind-induced ground-surface pressures increases dramatically as the soil permeability increases. In this flow, air enters the ground on the windward side of the house, and

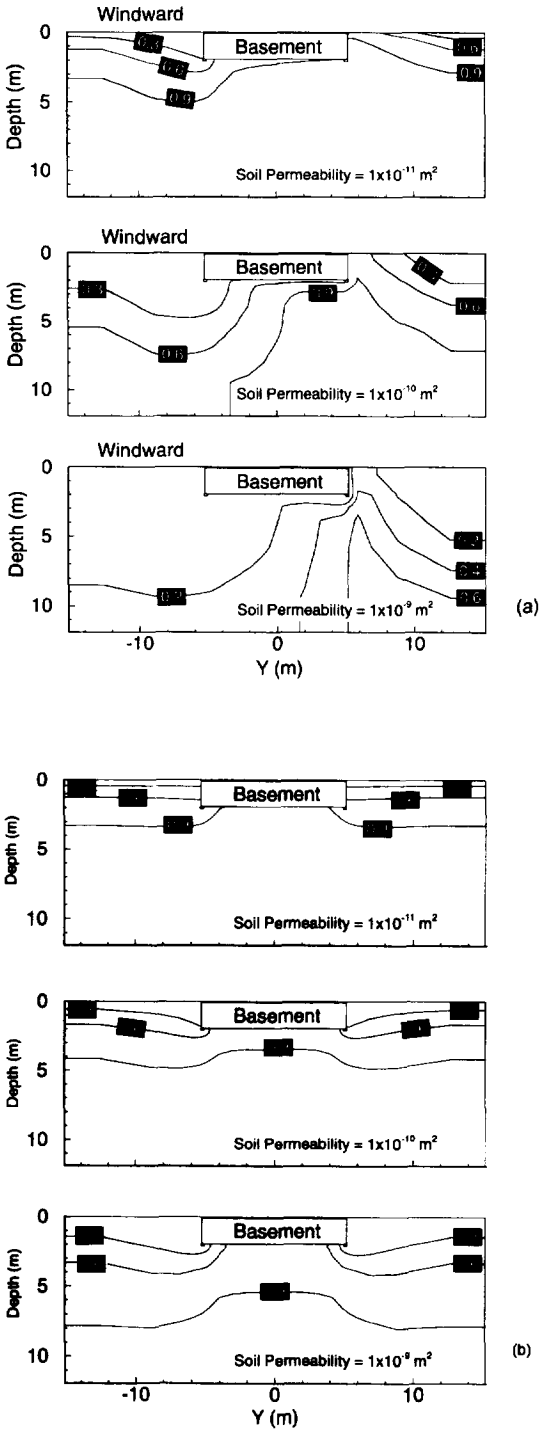

Fig. 5. Contour plots of soil-gas radon concentration at several soil permeabilities for the case of (a) an 8.3 m s^{-1} wind and (b) no wind. The concentration is normalized with respect to the deep-soil gas-phase radon concentration. Figures represent concentrations in a vertical plane bisecting the basement parallel to the long side of the house and the wind direction. As the soil permeability increases, the radon concentration in the soil gas adjacent to the slab decreases. Note the magnitude of the reduction in soil-gas radon concentration for the case with wind compared to the case with no wind. The basement depressurization is −11 Pa for both cases.

soil gas exits the ground surface on the other three sides of the building. The result is a significant flushing of radon from the soil gas beneath the house, and as a consequence, a diminished source for radon entry into the basement. In addition, because of the complex distribution of pressure on the ground surface there are unanticipated soil-gas flow patterns on the leeward side of the house.

Figure 5a shows normalized soil-gas radon concentrations in a vertical plane bisecting the soil block parallel to both the long side of the house and an 8.3 m s^{-1} wind. The dominant flow paths for the soil gas start from the soil surface on the left, proceed under the house, and exit from the soil surface on the right. For comparison, Fig. 5b shows the analogous contours of soil-gas radon concentration for the case without wind. The extent to which the wind flushes radon from soil gas is illustrated by comparing Figs 5a and b. It is apparent that, in the presence of wind, increasing soil permeability leads to sharply depressed levels of soil-gas radon in the vicinity of the footer-slab crack.

To quantify this effect, we define a characteristic soil-gas radon concentration, C_{char}, to represent the radon source available for entry into the basement. C_{char} is calculated by taking the area-weighted average of the radon concentration in a plane surface bounded by the lower interior edges of the footers. Figure 6 presents this parameter for the same four cases considered in Fig. 4. When there is no wind, C_{char} is not a sensitive function of soil permeability (Fig. 6a), and the result is a radon entry rate that generally follows the soil-gas flow rate into the basement. However, in the presence of wind, C_{char} decreases sharply with increasing soil permeability (Fig. 6b), leading to a decreasing radon entry rate. To summarize, the higher the soil permeability, the larger the extent of soil-gas flushing in the presence of a steady wind. The result is a lower available radon source, and therefore a lower radon entry rate.

Figure 7 shows soil-gas streamlines for an 8.3 m s^{-1} wind and a soil permeability of 3×10^{-9} m^2 in the same vertical plane used in Fig. 5. Notice the significant flow of soil gas that enters the gravel layer on the windward side of the house, moves through the gravel layer, and then exits on the leeward side. The high permeability gravel layer offers a preferred short-circuit path between the windward and leeward sides of the house. The second interesting (and unexpected) feature of the flow occurs in the soil region on the leeward side of the house, where soil gas is moving back toward the house. This peculiarity results because the leeward ground-surface pressure far from the house is larger than the pressure near the house (see Fig. 3a). Although the magnitude of the flow depends on soil permeability, the qualitative features shown here are fairly constant over the range of soil permeabilities and wind speeds examined.

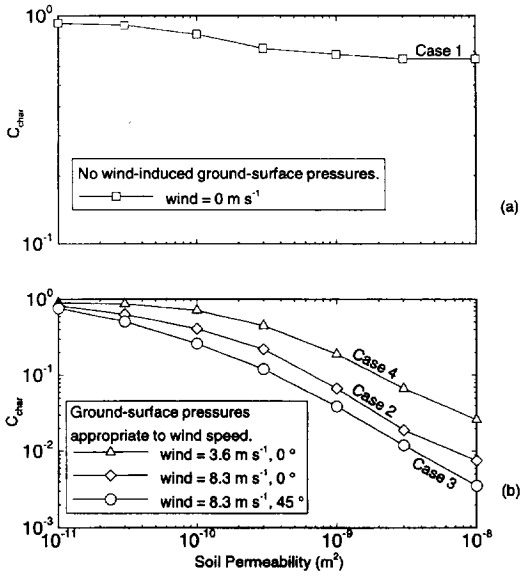

Fig. 6. Average radon soil-gas concentration (C_{char}) at a horizontal plane located at the bottom of the footers, and bounded by the footers. The concentration is normalized with respect to the deep-soil gas-phase radon concentration. The basement depressurization for no wind (i.e. no wind-induced ground-surface pressures) is set at -11 Pa, for the 3.6 m s^{-1} wind it is -2.0 Pa, and for the 8.3 m s^{-1} wind it is -11 Pa.

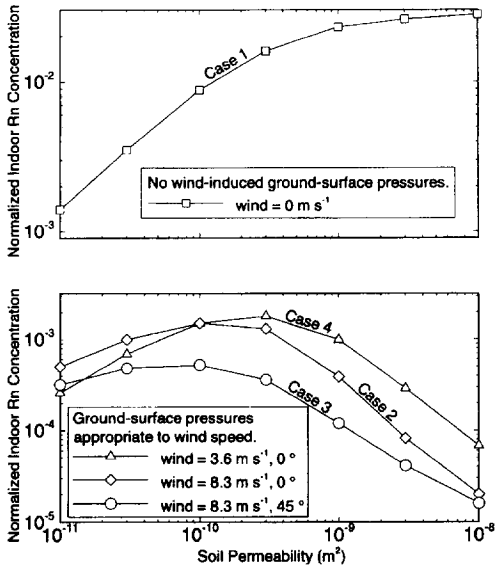

Fig. 8. Normalized indoor radon concentration as a function of wind speed and soil permeability. The basement depressurization for no wind (i.e. no wind-induced ground-surface pressures) is set at -11 Pa, for the 3.6 m s^{-1} wind it is -2.0 Pa, and for the 8.3 m s^{-1} wind it is -11 Pa.

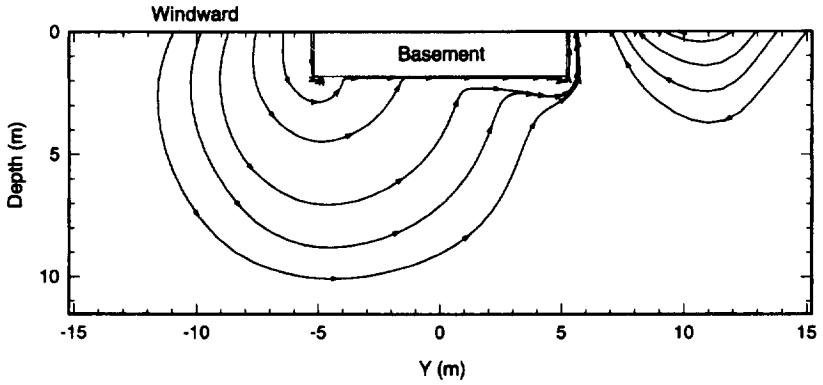

Fig. 7. Streamlines of gas flow through the soil and gravel layer. The wind speed is 8.3 m s^{-1}, the soil permeability is 3×10^{-9} m^2, and the gravel permeability is 3×10^{-7} m^2.

Indoor radon concentration

The calculated indoor radon concentration, C_{in}, is plotted as a function of wind speed and soil permeability in Fig. 8. Notice that the indoor radon concentration curves are similar in form to the radon entry rate curves shown in Fig. 4. Figures 4 and 8 suggest that a house exposed to a sustained wind will experience a substantial decrease in radon entry rate and indoor concentration, and that this decrease is a result not only of the increase in ventilation associated with the wind, but also of the concurrent flushing of radon from the soil gas in the vicinity of the house.

Experimental evidence of soil-gas flushing

One of the key predictions of our model is that the radon concentration in soil gas near a house can be depleted by wind-induced flushing. To explore whether this predicted behavior occurs in reality, we examined previously acquired data from a study of radon entry and mitigation in New Jersey (Turk *et al.*, 1991). The details of this investigation can be found in Riley *et al.* (1995b). For nine of the ten periods examined, the soil-gas radon concentration below the basement slab was observed to diminish in response to increasing wind. Although these experiments were not

sufficiently detailed to quantitatively validate our modeling results, they do support a key qualitative finding: that wind reduces soil-gas radon concentrations in the vicinity of a house.

CONCLUSIONS

Wind has a significant effect on radon entry rates and indoor concentrations in houses with basements. In addition to the well-established results that wind increases the building's ventilation rate and relative depressurization, soil-gas flow generated by wind-induced ground-surface pressures flushes radon from the soil near the house. The concentration of radon in the soil gas being drawn into the basement is thereby reduced; the result is a substantially lower radon entry rate. Since real houses are regularly exposed to wind, this effect must be included if radon entry is to be properly modeled.

The effect of ignoring wind-induced ground-surface pressures is illustrated by comparing the radon entry rates and indoor concentrations for cases 1 and 2 (Figs 4 and 8). In the absence of wind-induced ground-surface pressures (case 1), the radon entry rate and indoor concentration increase by an order of magnitude as the soil permeability increases from 10^{-11} to 10^{-8} m^2. However, including the effects of wind on ground-surface pressures (case 2) reduces the predicted radon entry rate relative to case 1 by a factor ranging from 3 at a permeability of 10^{-11} m^2 to 1000 at a permeability of 10^{-8} m^2. The predicted indoor concentrations differ between cases 1 and 2 by the same factors. Therefore, predictions concerning the effect of wind on indoor radon concentrations must include ground-surface pressures to avoid substantially errors, especially in regions having high soil permeability.

In addition to the cases presented here, we also conducted simulations with other ground-surface pressure fields (based on Scott's (1985) wind tunnel results and numerical simulation results from FLUENT), basement depressurizations, wind speeds, and wind angles. The effect of wind on the radon entry rate was found to be qualitatively the same as in the cases summarized here. We therefore conclude that, for this house geometry, the observed trends are robust.

The effect of a time-varying wind velocity on radon entry rates and indoor concentrations remains an unresolved issue. We are currently working to expand the capabilities of our NDSTAR model to analyze this scenario. Inclusion of time-varying soil-gas pressure, velocity, and concentration fields, in addition to a time-varying basement depressurization, will be necessary. The latter will be a function of both the fluctuating wind and the characteristics of the building shell, which will define how an external pressure is propagated throughout the house. Furthermore, an understanding of the effects of transient winds on radon entry is expected to be important in the design of passive or low-energy mitigation systems where a direct connection between the atmosphere and the subslab gravel layer may be present (Fisk *et al.*, 1995).

Further work is also required to determine the effect of wind on the radon entry rate into houses with different geometries (e.g. L-shaped or split-level homes) and high-rise buildings. Such buildings may respond differently than predicted here because of differences in the wind-induced ground-surface pressure field.

In summary, we have found the effects of a steady wind on radon entry rates and indoor radon concentrations to be substantial. Accounting only for the increase in building depressurization and ventilation is insufficient to predict the effect of wind on indoor radon concentrations. The concurrent flushing of radon from the soil gas that is driven by wind-generated ground-surface pressures must also be considered. Further study of the effects of wind on radon entry (i.e. considering transient winds and different building geometries) is necessary to complete our understanding of this phenomenon and enable us to design mitigation systems that can most efficiently reduce human exposures to indoor radon.

Acknowledgements—This work was supported by the Assistant Secretary for Conservation and Renewable Energy, Office of Building Technologies, Building Systems and Materials Division and by the Director, Office of Energy, Office of Health and Environmental Research, Human Health and Assessments Division and Pollutant Characterization and Safety Research Division of the U.S. Department of Energy under Contract No. DE-AC03-76SF00098. Additional support was provided by the National Science Foundation through grant BCS-9057298. The authors wish to thank Bill Fisk for many helpful conversations. Also, the authors wish to thank Phil Price, Ken Revzan, and Rich Sextro for their thorough review of the manuscript.

REFERENCES

Arnold L. J. (1990) A scale model study of the effects of meteorological, soil, and house parameters on soil gas pressures. *Health Phys.* **58,** 559–573.

Baker P. H., Sharples S. and Ward I. C. (1987) Air flow through cracks. *Bldg. Envir.* **22,** 293–304.

Bauman F. S., Ernest D. R. and Arens E. A. (1988) ASEAN natural ventilation study: wind pressure distributions on long building rows in urban surroundings. CEDR-03-88, Center for Environmental Design Research, University of California, Berkeley, California.

Bonnefous Y. C., Gadgil A. J., Fisk W. J., Prill R. J. and Nematollahi A. R. (1992) Field study and numerical simulation of subslab ventilation systems. *Envir. Sci. Technol.* **26,** 1752–1759.

Feustel H. E. (1985) Development of a simplified multizone infiltration model. LBL-19005, Lawrence Berkeley Laboratory, Berkeley, California.

Fisk W. J., Prill R. J., Wooley J., Bonnefous Y. C., Gadgil A. J. and Riley W. J. (1995) New methods of energy efficient radon mitigation. *Health Phys.* **68,** 689–698.

FLUENT (1993) v4.2, Fluent Incorporated, Centerra Resource Park, 10 Cavendish Court, Lebanon, New Hampshire, 03766.

Gadgil A. J., Bonnefous Y. C., Fisk W. J., Prill R. J. and Nematollahi A. (1991) Influence of subslab aggregate permeability on SSV performance. LBL-31160, Lawrence Berkeley Laboratory, California.

Mowris R. J. and Fisk W. J. (1988) Modeling the effects of exhaust ventilation on ^{222}Rn entry rates and indoor ^{222}Rn concentrations. *Health Phys.* **54,** 491–501.

Nazaroff W. W. (1992) Radon transport from soil to air. *Rev. Geophys.* **30,** 137–160.

Nazaroff W. W., Feustel H., Nero A. V., Revzan K. L. and Grimsrud D. T. (1985) Radon transport into a detached one-story house with a basement. *Atmospheric Environment* **19,** 31–46.

Nazaroff W. W., Moed B. A. and Sextro R. G. (1988) Soil as a source of indoor radon: generation, migration, and entry. In *Radon and its Decay Products in Indoor Air* (edited by Nazaroff W. W. and Nero A. V.), pp. 57–112. Wiley, New York.

NOAA (1980) National Oceanic and Atmospheric Administration. Local climatological data, annual summaries for 1980, Part II—NEB—WYO, National Climatic Center, Asheville, North Carolina, 28801.

Owczarski P. C., Holford D. J., Burk K. W., Freeman H. D. and Gee G. W. (1991) Effect of winds in reducing sub-slab radon concentrations under houses laid over gravel beds. In the 1991 Int. Symp. on Radon and Radon Reduction Technology: Vol. 3, Philadelphia, Pennsylvania, U.S. EPA, Air and Energy Environmental Research Laboratory, Research Triangle Park, North Carolina.

Palmiter L. and Brown I. (1989) Northwest residential infiltration study, Vol. I: Analysis and results. Prepared for the Bonneville Power Admin. (U.S. Dept. of Energy), DOE/BP-34625-1.

Patankar S. V. (1980) *Numerical Heat Transfer and Fluid Flow.* Hemisphere Publishing, New York.

Revzan K. L. and Fisk W. J. (1992) Modeling radon entry into houses with basements: the influence of structural factors. *Indoor Air* **2,** 40–48.

Riley W. J., Gadgil A. J. and Nazaroff W. W. (1995a) Wind-induced ground-surface pressures around a single family house. *J. Wind Eng. Ind. Aerodyn.* (submitted).

Riley W. J., Gadgil A. J., Bonnefous Y. C. and Nazaroff W. W. (1995b) The effect of steady winds on radon entry into houses, LBL-36372, Lawrence Berkeley Laboratory, Berkeley, California.

Scott A. G. (1985) A computer model study of soil gas movement into buildings. Report No. 1389/1333, Department of Health and Welfare, Ottawa, Ontario, Canada.

Sherman M. H., Wilson D. J. and Kiel D. E. (1984) Variability in residential air leakage. Proc. Symp. on Measured Air Leakage Performance of Buildings, Philadelphia, Pennsylvania, The American Society for Testing and Materials.

Sherman M. H. (1992) Simplified modeling for infiltration and radon entry. LBL-31305, Lawrence Berkeley Laboratory, Berkeley, California.

Turk B. H., Prill R. J., Grimsrud D. T., Moed B. A and Sextro R. G. (1990) Characterizing the occurrence, sources, and variability of radon in Pacific northwest homes. *J. Air Waste Man. Assoc.*, **40,** 498–506.

Turk B. H., Harrison J. and Sextro R. G. (1991) Performance of radon control systems. *Energy Bldg.* **17,** 157–175.

Van der Hoven I. (1957) Power spectrum of horizontal wind speed in the frequency range from 0.0007 to 900 cycles per hour. *J. Met.* **14,** 160.

Ward D. C., Borak T. B. and Gadd M. S. (1993) Characterization of ^{222}Rn entry into a basement structure surrounded by low permeability soil. *Health Phys.* **65,** 1–11.